

Exciton transport in amorphous polymers and the role of morphology and thermalisation

Francesco Campaioli^{1,*} and Jared H. Cole^{1,†}

¹*Chemical and Quantum Physics, and ARC Centre of Excellence in Exciton Science,
School of Science, RMIT University, Melbourne 3000, Australia*

(Dated: February 5, 2022)

Understanding the transport mechanism of electronic excitations in conjugated polymers is key to advancing organic optoelectronic applications, such as solar cells, OLEDs and flexible electronics. While crystalline polymers can be studied using solid-state techniques based on lattice periodicity, the characterisation of amorphous polymers is hindered by an intermediate regime of disorder and the associated lack of symmetries. To overcome these hurdles we use a reduced state quantum master equation approach based on the Merrifield exciton formalism. Using this model we study exciton transport in conjugated polymers and its dependence on morphology and temperature. Exciton dynamics consists of a thermalisation process, whose features depend on the relative strength of thermal energy, electronic couplings and disorder, resulting in remarkably different transport regimes. By applying this method to representative systems based on poly(p-phenylene vinylene) (PPV) we obtain insight into the role of temperature and disorder on localisation, charge separation, non-equilibrium dynamics, and experimental accessibility of thermal equilibrium states of excitons in amorphous polymers.

I. INTRODUCTION

Organic semiconductors (OSCs) are at the forefront of the current research efforts for the development and improvement of optoelectronic technology, such as solar cells [1–3], organic light-emitting diodes (OLEDs) [4, 5], thin-film transistors [6–9], sensors and flexible electronics [10–13]. In particular, conjugated polymers are a key class of OSCs for photovoltaic applications, due to their ability to transport electronic excitations, i.e., *excitons*, over tens of nanometers, together with their low production cost, ease of fabrication and flexibility [14, 15]. Depending on their chemical composition and fabrication conditions, polymeric semiconductors can be found in a variety of different morphologies characterised by specific exciton transport properties [16].

While the fundamental features of energy and charge transport across crystalline, semicrystalline and amorphous polymers are qualitatively known, the dependence of exciton dynamics on temperature and morphology is still an important area of investigation [17–20]. For example, the introduction of amorphous polymers characterised by high electron mobility has challenged the idea that crystalline ones would be optimal for charge transport [21–26]. The study of exciton transport in amorphous polymers is however hindered by the complexity that arises from their disordered nature, which prevents the use of solid-state techniques based on lattice periodicity. In this intermediate transport regime between band conduction and incoherent hopping, semiclassical techniques such as Marcus theory often fail to reproduce the coherent quantum attributes of the exciton dynamics [27–30], while first-principles calculations like multiconfiguration time-dependent Hartree method (MCTDH) become computationally intractable due to the large size of the systems of interest [19, 20, 31–34].

An effective alternative to study exciton transport in disordered OSCs is given by reduced state quantum master

equations [15]. These allow for the efficient description of the interaction between excitons and nuclear vibrations, i.e., *phonons*, and account for both coherent and incoherent dynamics. Quantum master equations have therefore been applied to a variety of exciton transport problems in OSCs, such as natural photosynthetic complexes [35–38], molecular aggregates [39–42], and disordered systems [34, 43]. A key insight from this body of literature is that exciton-phonon interactions have an essential role for exciton transport in OSCs. On one hand, decoherence induced by local and uncorrelated phonon modes is known to improve transport efficiency in disordered systems [36, 44, 45], counteracting weak and strong localisation phenomena, such as Anderson localisation [46–49], that otherwise prevail when dynamics is primarily coherent. On the other hand, strong spatial correlations between bath modes can facilitate the emergence of decoherence-free subspaces, improving transport of certain states in ordered systems [50].

Recently, quantum master equations have also been used to study exciton transport in conjugated polymers, albeit only for the case of crystalline morphologies. In Ref. [19], Lyskov *et al.* bridge first-principles calculations to a Lindblad master equation [51–55], and obtain a phenomenological model for triplet exciton dynamics in crystalline poly(p-phenylene vinylene) (PPV). Their results show that, conversely to the case of disordered OSCs, decoherence slows down exciton dynamics in crystalline PPV, inducing a rapid transition from ballistic (coherent) to diffusive (incoherent) transport. However, the model used in Ref. [19] cannot be directly applied to amorphous polymers, whose difficult theoretical characterisation presents several questions [33, 56–67]. How do temperature and morphology affect exciton transport? What are the features of the dynamical transition between localised and delocalised states? Are thermal equilibrium states experimentally accessible? How does disorder affect charge-separation dynamics?

Here we answer these questions generalising the master equation approach used in Ref. [19] to conjugated polymers with arbitrary morphology. Firstly, since excited electronic states of amorphous polymers are known to display charge

* francesco.campaioli@rmit.edu.au

† jared.cole@rmit.edu.au

separation over a few monomers [24, 26], we formulate a master equation for the dynamics of Merrifield excitons [31, 68], i.e., a strongly coupled electron-hole pair. Accordingly, our approach can be seen as a direct extension of the master equations used in Refs. [19, 36–38] for the dynamics of charge-neutral Frenkel excitons [69], characteristic of OSCs with low dielectric constant.

Furthermore, our model, introduced in Sec. II, provides a rigorous thermodynamic description of exciton-phonon interactions, overcoming the limitations of the phenomenological approach used in Ref. [19]. There, the authors fit the master equation parameters to MCTDH calculations carried out on small two-monomer subsystems over short time scales. Such approach, affected by artificially short recurrence times, may fail to correctly reproduce the dynamics for long time scales and returns decoherence rates that do not necessarily obey thermodynamics in the long-time limit. Here, instead, we use the Bloch-Redfield formalism to calculate temperature-dependent decoherence rates from the phonons' correlation functions [53, 70], to then express the dynamics of the exciton's reduced state using a master equation of the Lindblad form [35, 40–42, 54]. This approach has the additional advantage of providing ensemble average transport properties without calculating many individual stochastic realisations of system-environment dynamics.

In Sec. III, we use the model to study the exciton transport properties of some representative oligo and poly(p-phenylene vinylene) (OPV and PPV) systems, across different morphologies, from crystalline to highly disordered. Instead of relying on material-specific modelling of polymers, we express our calculations in terms of electronic couplings and thermal energy. This allows us to explore the impact that disorder and temperature have on localisation, charge-separation dynamics and equilibration time scales. Exciton transport is therefore interpreted as a thermalisation process [53, 54, 70–73], whose features vary with the relative strength between thermal energy, electronic couplings and disorder. We show how such differences in electronic coupling determine whether the phonon bath *cools* or *heats* the system, with dramatic effects on exciton transport properties. We conclude discussing our results in Sec. IV, where we compare and contrast our findings with those of other works, and outlining the use of our method to exciton transport problems of great importance for optoelectronic applications.

II. METHODOLOGY

The exciton transport model that we introduce in this article is based on the following two premises. First, the characteristic times and energies associated with exciton transport in OSCs at room temperature and natural illumination imply that excitons do not interact with each other, as they are sufficiently spatially and temporally separated [15]. Under these circumstances, it is a standard approach to focus on the transport of a single electronic excitation, formally defined by the single-exciton manifold [15, 19, 20, 31, 36–38]. Second, we consider polymeric materials whose structural changes are far slower

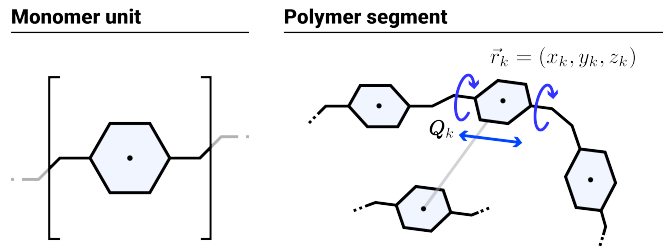


FIG. 1. Polymeric materials are here modelled as a network of N nodes, each of which represents a monomer. Monomers positions \vec{r}_k and conformational coordinates Q_k define the morphology of the medium and the structure of the exciton's Hamiltonian. Exciton transport on such network is mediated by through-bond couplings between conjugated monomers that are part of the same polymer, or by through-space couplings (*gray line*) between pairs of monomers in proximity of each other.

than the characteristic femtosecond to nanosecond time scales of exciton dynamics, such as for the paradigmatic case of PPV and its amorphous derivative MEH-PPV [24, 26]. This allows us to adopt a snapshot approach for a medium's morphology, which is assumed to be time-independent. Additionally, we assume that the interaction between excitons and rapidly oscillating conformational coordinates like bond-length alternations, here modelled as a bath of independent harmonic oscillators, are well described in the weak coupling approximation [15, 35].

Under these assumptions, the transport of a single electronic excitation in OSCs is typically modelled as a *quantum stochastic walk* (QSW) of a charge-neutral Frenkel exciton over a network of N nodes [74, 75], each of which represents a monomer or a chromophore [15, 19, 35, 37]. However, motivated by recent results on the electronic excitations of amorphous polymers [24, 26], we here generalise this standard approach and extend the dynamics to charge-separated exciton states using the Merrifield model [31]. In this formalism the states of the single-exciton manifold are here given by the product of the localised single-electron and single-hole bases,

$$\mathcal{B} := \{|jk\rangle\}_{j,h=1}^N, \quad (1)$$

where $|jk\rangle := |j\rangle_e \otimes |k\rangle_h$, and where $|j\rangle_e$ ($|k\rangle_h$) represents the state of the electron (hole) localised on monomer j (k) of a polymeric material. Every monomer k is also associated with its centre's position $\vec{r}_k := (x_k, y_k, z_k)$ and a set of local conformational coordinates Q_k , such as torsional angles and bond-length alternations, as schematically represented in Fig. 1. These, together with the bonds between pairs of monomers, define the *morphology* of the medium and determine the structure of the exciton's Hamiltonian, as described in the next section.

A. Exciton Hamiltonian

The exciton Hamiltonian $H_{\text{ex}} = H_0 + H_F + H_{\text{CT}}$ is given by the Coulomb term H_0 , which defines the energetic landscape

associated with electron-hole configurations on the polymeric material, and the Frenkel H_F and charge H_{CT} transfer terms, which model the coherent transport of energy and charges, respectively. In the electron-hole basis of Eq. (1), the Coulomb term H_0 reads

$$\langle eh|H_0|e'h'\rangle = \delta_{ee'}\delta_{hh'}\left(E_0 - \frac{1}{4\pi\epsilon_0\epsilon_r d_{eh}}\right), \quad (2)$$

where $E_0^{-1} = (4\pi\epsilon_0\epsilon_r r_0)$ is the exciton binding energy of electron-hole pairs that are localised within the same monomers, i.e., Frenkel excitons. The electron-hole distance, $d_{eh} = r_0 + \|\vec{r}_e - \vec{r}_h\|$, is obtained from the distance between two monomers offset by the intrinsic electron-hole distance r_0 for Frenkel excitons in the considered polymer [31]. The Coulomb term is diagonal in the electron-hole basis, and vanishes for Frenkel excitons. The morphology of the medium introduces static disorder in this term via the inter-monomer distance d_{eh} .

The Frenkel term H_F models the coherent transport of Frenkel excitons and is given by

$$\langle eh|H_F|e'h'\rangle = \delta_{eh}\delta_{e'h'}V_F(\vec{r}_e, \mathbf{Q}_e; \vec{r}_{e'}, \mathbf{Q}_{e'}), \quad (3)$$

where $V_F(\vec{r}_j, \mathbf{Q}_j; \vec{r}_k, \mathbf{Q}_k)$ is the strength of the Frenkel coupling between a pair of monomers j, k , as a function of the morphology of the medium. Frenkel transfer terms preserve charge separation, and can only mediate the transport of Frenkel exciton states, which form a N dimensional subset of the full N^2 dimensional Hilbert space associated with the single-exciton manifold of the Merrifield model.

Similarly, the charge transfer (CT) term H_{CT} models the coherent transport of individual charges and is given by

$$\langle eh|H_{CT}|e'h'\rangle = \delta_{ee'}V_{CT}(\vec{r}_h, \mathbf{Q}_h; \vec{r}_{h'}, \mathbf{Q}_{h'}) + \delta_{hh'}V_{CT}(\vec{r}_e, \mathbf{Q}_e; \vec{r}_{e'}, \mathbf{Q}_{e'}), \quad (4)$$

where $V_{CT}(\vec{r}_j, \mathbf{Q}_j; \vec{r}_k, \mathbf{Q}_k)$ represents the strength of the CT coupling between a pair j, k of monomers, as a function of the morphology of the medium. The CT term can map Frenkel states into charge-separated states and vice versa, and its addition to the Hamiltonian allows exciton states to explore the entirety of the single-exciton manifold.

The dependence of the coupling strengths V_F and V_{CT} on the morphology of the medium is described in terms of the relative arrangement of pairs of monomers that are conjugated, or close enough to each other to allow for weaker through-space couplings. Without loss of generality, V_F and V_{CT} are assumed to be symmetric in the pairs' indices and to vanish for monomers that are not connected by a bond, or out of range for through-space interactions. An example of the dependence of V_F and V_{CT} on the morphology for PPV-like conjugated polymers is given by Eqs. (14) and (15) in Sec. III.

B. Exciton-phonon interaction

Exciton-phonon interactions induce decoherence and relax the exciton states until a steady state is reached. The composite

dynamics of exciton and phonons is governed by the system-environment Hamiltonian $H = H_{\text{ex}} + H_{\text{ex-ph}} + H_{\text{ph}}$. The vibrational modes involved in this process, such as bond-length alternations and ring-breathing modes [19, 24, 26], are modelled as a bath of local and independent harmonic oscillators [15, 19]. Let us write the exciton-phonon interaction Hamiltonian $H_{\text{ex-ph}}$ as

$$H_{\text{ex-ph}} = \sum_l A_l \otimes B_l, \quad (5)$$

such that each coupling operator A_l acting on the exciton space is associated with a bath operator

$$B_l = \sum_m g_{l,m} (b_{l,m}^\dagger + b_{l,m}) \quad (6)$$

given by a sum over the displacement operators associated with the modes with frequencies $\omega_{l,m}$, written in terms of creation and annihilation operators. The tensor $g_{l,m}$ represents the coupling strengths between the modes $\omega_{l,m}$ and the exciton coupling operators A_l . These are assumed to be *weak*, with respect to the characteristic energies of H_{ex} and H_{ph} . In this notation the phonon Hamiltonian reads

$$H_{\text{ph}} = \sum_{l,m} \hbar \omega_{l,m} \left(b_{l,m}^\dagger b_{l,m} + \frac{1}{2} \right). \quad (7)$$

The exciton coupling operators A_l model the exchange of energy between the exciton and the vibrational modes. These can either involve a single monomer, or a bond between two monomers. For example, the interaction between a Frenkel state $|kk\rangle\langle kk|$ and ring-breathing modes concerns an individual monomer, here labelled by k . Conversely, the interaction between Frenkel transfer terms $|jj\rangle\langle kk| + h.c.$ and bond-length alternation modes is associated with the bond between a pair j, k of monomers. The set of exciton coupling operators A_l considered in this model is given in Table I.

C. Master equation

The dynamics of the reduced exciton state ρ_t is governed by a Lindblad master equation [76] that is obtained from the system-environment Hamiltonian H by tracing over the phonon environment [53]

$$\begin{aligned} \dot{\rho}_t = & -\frac{i}{\hbar}[H_{\text{ex}}, \rho_t] + \sum_{\omega,l} \gamma_l(\omega) \left(A_l(\omega) \rho_t A_l^\dagger(\omega) + \right. \\ & \left. + \frac{1}{2} \left\{ A_l^\dagger(\omega) A_l(\omega), \rho_t \right\} \right). \end{aligned} \quad (8)$$

The Lindblad collapse operators $A_l(\omega)$ are here given by the spectral representation of the coupling operators A_l ,

$$A_l(\omega) = \sum_{E_{\lambda'} - E_{\lambda} = \omega} |E_{\lambda}\rangle\langle E_{\lambda}| A_l |E_{\lambda'}\rangle\langle E_{\lambda'}|, \quad (9)$$

where $|E_\lambda\rangle$ are the eigenstates of the exciton Hamiltonian, $H_{\text{ex}}|E_\lambda\rangle = E_\lambda|E_\lambda\rangle$, such that ω matches the Bohr frequencies $E_{\lambda'} - E_\lambda$. The relaxation rates $\gamma_l(\omega)$ are obtained from the Fourier transform of the bath correlation functions $\langle B_l(t)B_{l'}(t') \rangle = \text{Tr}[B_l(t)B_{l'}(t')\rho_{\text{ph}}]$ [53, 54]. Here, $\rho_{\text{ph}} = \exp(-\beta H_{\text{ph}})\mathcal{Z}^{-1}$ is the steady state of the phonon bath, in thermal equilibrium at inverse temperature $\beta = (k_B T)^{-1}$, with partition function $\mathcal{Z} = \text{Tr}[\exp(-\beta H_{\text{ph}})]$ [54].

This general approach, also known as the Bloch-Redfield formalism, allows to obtain relaxation rates from the energy and temperature dependent correlation functions of the bath. The rates obtained this way satisfy thermodynamics and detailed balance condition, leading to the correct thermal equilibrium distribution for long time scales [70]. Here, we obtain a prescription for the dynamics of exciton states in the Markovian approximation, under which condition the master equation can be equivalently expressed in either Bloch-Redfield or Lindblad formalism [70].

In the Markovian limit that characterises Eq. (8), the bath correlation functions only depend on the time interval τ between two time steps $t - t' = \tau$ [53, 54]. Moreover, in virtue of the mutual independence of the vibrational modes for each pair of coupling operators $A_l, A_{l'}$, the bath correlation functions reduce to

$$\langle B_l(\tau)B_{l'}(0) \rangle = \delta_{ll'} \sum_m g_{l,m}^2 \left((1 + \nu_\beta(\omega_{l,m})) e^{-i\omega_{l,m}\tau} + \nu_\beta(\omega_{l,m}) e^{i\omega_{l,m}\tau} \right), \quad (10)$$

where $\nu_\beta(\omega) = (\exp(\hbar\beta\omega) - 1)^{-1}$ is the bosonic distribution function at inverse temperature β [53, 54].

To calculate the rates $\gamma_l(\omega)$, the sum over the couplings $g_{l,m}$ of Eq. (10) is replaced with an integral in the frequency domain, $\sum_m g_{l,m}^2 \rightarrow \int J_l(\omega) d\omega$, where $J_l(\omega)$ is a spectral density that can be used to sample the coupling strengths $g_{l,m}$. To do so we use an Ohmic spectral density $J_l(\omega)$

$$J_l(\omega) = \frac{\Lambda_l}{\hbar} \frac{\omega}{\Omega_l} \exp\left(-\frac{\omega}{\Omega_l}\right), \quad (11)$$

where $\Lambda_l = \hbar \int_0^\infty d\omega J_l(\omega)/\omega$ is the reorganisation energy associated with coupling operator A_l [35, 53]. In this way the relaxation rates read

$$\gamma_l(\omega) = 2\pi \left(J_l(\omega)(1 + \nu_\beta(\omega)) + J_l(-\omega)\nu_\beta(-\omega) \right). \quad (12)$$

Exciton-phonon interactions also introduce further disorder, which is captured by energy fluctuations δE_l in the exciton Hamiltonian, $H_{\text{ex}} \rightarrow H_{\text{ex}} + \sum_l \delta E_l A_l$ [34, 43]. These are sampled from a normal distribution with zero average and standard deviation $\sigma_l(\beta)$, given by

$$\sigma_l^2(\beta) = \int_0^\infty d\omega \hbar J_l(\omega) \coth\left(\frac{\hbar\beta\omega}{2}\right), \quad (13)$$

as done in Ref. [42, 77]. The addition of such energy fluctuations affects site energies and coherent transfer terms, leading

Exciton coupling operators (A_l)		
	Site k	Bonds j, k
Frenkel	$ kk\rangle\langle kk $	$ jj\rangle\langle kk + h.c.$
Electron	$ k\rangle\langle k _e \otimes \mathbb{1}_h$	$(j\rangle\langle k _e + h.c.) \otimes \mathbb{1}_h$
Hole	$\mathbb{1}_e \otimes k\rangle\langle k _h$	$\mathbb{1}_e \otimes (j\rangle\langle k _e + h.c.)$

TABLE I. Exciton coupling operators A_l classified by their action on Frenkel, electron, and hole states and transfer terms.

to asymmetry in the charge separation landscape and promoting localisation in the centre of mass dynamics [49, 78, 79].

In the next section we use Eq. (8) to study exciton transport in conjugated polymers across different morphologies. Before discussing the results, let us make a few remarks on the approximations that characterise Eq. (8). First of all, it is worth pointing out that, in Eq. (8) we have neglected the Lamb-Shift Hamiltonian term. This term accounts for the contributions of the coupling operators A_l to the coherent dynamics of the exciton. Lamb-Shift corrections have often been neglected in exciton transport problems, especially for the case of local and uncorrelated phonon baths [35, 37, 38]. When applying Eq. (8) in Sec. III we will assume the exciton Hamiltonian to already include energy shift arising from the weak coupling with the phonon environment. There, Lamb-Shift corrections are expected to be well below the precision limit of a qualitative study focused on order-of-magnitude differences in exciton energies and electronic couplings.

Another important observation is that we have assumed the vibrational modes to be uncoupled with each other, which is the reason why Eq. (8) does not feature combinations of $A_l(\omega)$ and $A_{l'}(\omega)$ Lindblad operators. It is reasonable to imagine that this approximation would not be justified for some combinations of coupling operators, such as for those vibrational modes coupled with the same monomer. When spatial correlations become important, e.g., when phonon modes are delocalised over several monomers, they can be simply accounted for and included into Eq. (8) via the addition of terms in A_l and $A_{l'}$, and the associated rates arising from the spatial dependence of the correlation functions $\langle B_l(t), B_{l'}(0) \rangle$ [80]. The presence of strong and long-range spatial correlations allows for the formation of decoherence free subspaces and gives rise to super and subradiance phenomena [81], which have been studied for biological light-harvesting complexes [70], but remain rather unexplored for the case of organic polymers.

Finally, the weak coupling approximation for the exciton-phonon interaction, necessary to obtain Eq. (8), is arguably the main source of deviations from a rigorous description of the exciton transport. While some vibrational modes, such as those associated with torsional angles and foldings of a polymer chain, are very likely to be well described by a weak coupling approximation, others modes, such as bond-length alternations, can couple strongly with the excitons. In such cases it is possible to overcome the limitations imposed by Eq. (8) by performing a polaron-transformation [82–85], which models the dynamics of an exciton followed by nuclear deformations,

Exciton Hamiltonian parameters — OPV, PPV		
Parameter		Hartree AU
Frenkel electron-hole distance	r_0	12.7
Exciton binding energy	E_0	7.90×10^{-2}
Frenkel transfer parameters	j_0	5.03×10^{-3}
	j_2	1.20×10^{-2}
	j_4	3.23×10^{-2}
Charge transfer parameter	t_0	9.78×10^{-2}
Relative permittivity	ϵ_0	1

TABLE II. Exciton Hamiltonian parameters used in Eqs. (2), (14), and (15) for the OPV and PPV-like materials considered in Secs. III A and III B, expressed in Hartree atomic units [31]. Frenkel transfer parameters have been scaled in Sec. III C in order to study the dependence of transport properties on the strength of the electronic couplings.

i.e., a polaron (or *dressed-exciton*), using master equations similar to Eq. (8), such as the secular polaron-transformed Redfield equation (sPTRE) [33, 34, 43, 86–91].

III. RESULTS

We now use Eq. (8) to study room-temperature exciton transport in some representative conjugated oligomers and polymers, exploring the transition from ordered to disordered morphologies. To compare our findings with previous results, we base our calculation upon the electronic properties of OPV and PPV, used in Refs. [19, 31]. In particular, we focus on the following systems. First, we consider a short OPV hexamer to explore centre of mass (CoM) and charge separation (CS) dynamics with a full Merrifield exciton approach, in Sec. III A. Then, in Sec. III B, we model a long PPV polymer with 51 repeated unit to explore intrachain Frenkel exciton dynamics across different morphological regimes. Finally, we examine the role of intrachain and interchain transport and its dependence on electronic coupling strength in Sec. III C, by looking at Frenkel exciton transport in OPV oligomers.

The different regimes of disorder, from *crystalline* to *amorphous*, are here achieved sampling torsional angles and bond length-alternations from a normal distribution with zero average and tunable standard deviation. The functional dependence of Frenkel and CT terms on the relative arrangement between two conjugated monomers, given by $V_F(d, \theta) = f(d)\Theta_F(\theta)$ and $V_{CT}(d, \theta) = f(d)\Theta_{CT}(\theta)$, respectively, is calculated upon their distance d and the relative angle θ between the two monomers' planes. The angular dependence $\Theta_F(\theta)$ and $\Theta_{CT}(\theta)$ is modelled as in Ref. [31],

$$\Theta_F(\theta) = (j_4 - j_0) \cos^4 \theta + (j_2 - j_0) \cos^2 \theta - 2j_0, \quad (14)$$

$$\Theta_{CT}(\theta) = t_0 \cos \theta, \quad (15)$$

while the dependence on the intra-monomer distance is heuristically modelled with a Gaussian factor $f(d) = \exp[-(d - r_0)^2 / 4r_0^2]$.

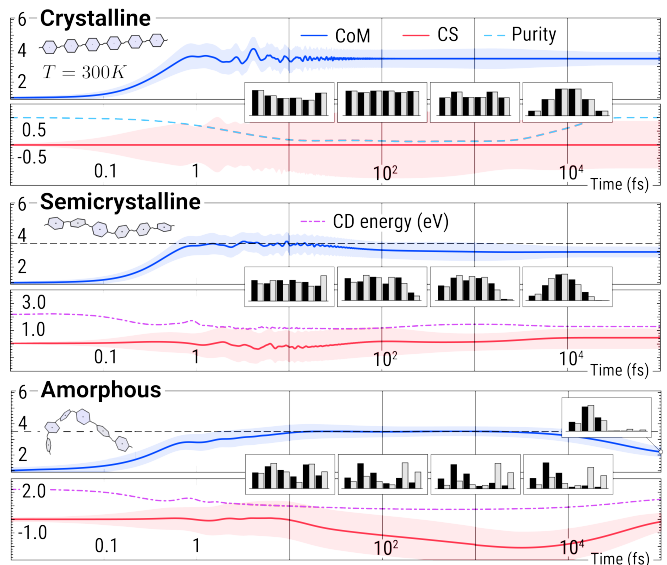


FIG. 2. Exciton transport for different instances of OPV hexamer morphologies at room temperature $T = 300K$. For each case the initial state ρ_0 is a Frenkel exciton localised on the first monomer. Expectation value (solid lines) and standard deviation (shaded areas) of CoM (blue) and CS (red) are expressed in the sites basis. The energy required for charge dissociation (dotted-dashed magenta line) is shown in eV (on the same y -axis as CS). The histograms insets schematically represent the populations (not in scale) of the partial states of electron (black bars) and hole (light gray bars) on each site at a given time.

The parameters used in Eqs. (2), (14), and (15) are given in Tab. II and expressed in Hartree atomic units, while the relative permittivity of the considered materials is assumed to be $\epsilon_r = 1$ for simplicity. The characteristic electronic couplings associated with Frenkel and charge-transfer terms can be as high as 2 eV, and, thus, much larger than the 26 meV associated with the thermal energy of the phonon bath at room temperature of 300K. When required, Frenkel through-space couplings are included for non-conjugated monomers that are separated by $\approx r_0$, with characteristic energies around 10 meV [19, 92].

Reorganisation energies Λ_l and cut-off frequencies Ω_l associated with vibrational modes define relaxation rates $\gamma_l(\omega)$ and energy fluctuations $\sigma_l(\beta)$, as prescribed by Eq. (11) [53, 54]. For the considered systems we have chosen reorganisation energies of 500 meV and 50 meV for monomer-local and bond-local vibrational modes, respectively. The chosen cut-off frequencies are 1500 cm^{-1} for modes that couple with Frenkel states, 1000 cm^{-1} for modes that couple with individual charges and Frankel transfer terms, and 500 cm^{-1} for modes that couple with CT terms [19, 32, 93, 94].

To propagate an initial exciton state ρ_0 we exactly solve the system of linear differential equations associated with Eq. (8) written in Liouville space [95]. In this way we obtain a map Λ_t for the dynamics of the state $\rho_t = \Lambda_t[\rho_0]$. Exciton transport properties are studied evaluating time-dependent expectation value and standard deviation of CoM and CS operators. These can be expressed in terms of monomer indices

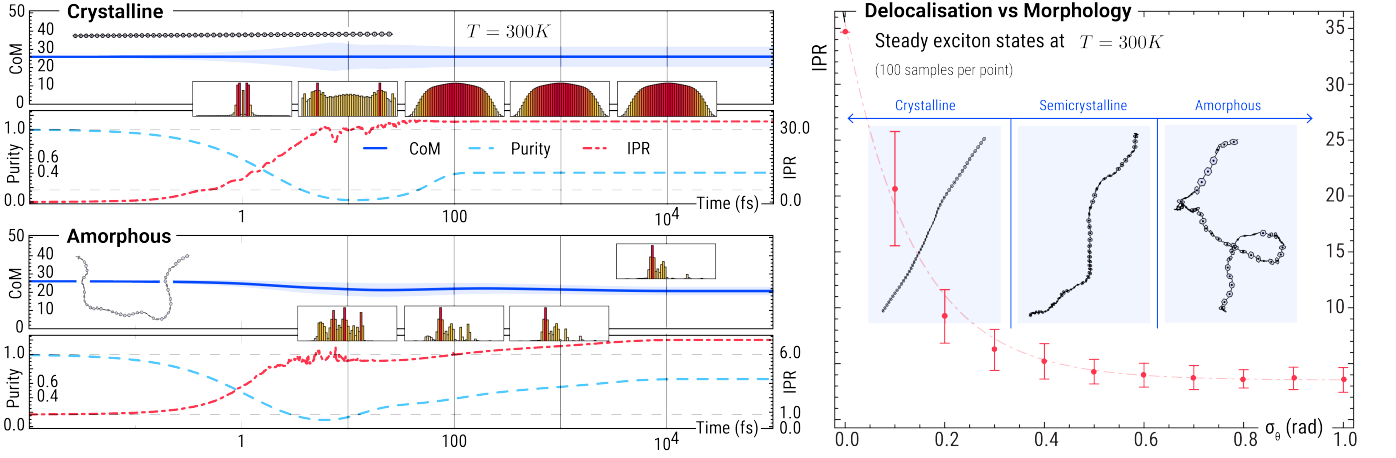


FIG. 3. (Left) Exciton transport for crystalline (top-left) and amorphous (bottom-left) PPV polymers with 51 monomers, at room temperature $T = 300K$. For each case the initial state ρ_0 is a Frenkel exciton localised on the central monomer ($k = 26$). Expectation value (solid lines) and standard deviation (shaded areas) of CoM (blue) are expressed in the sites basis. Delocalisation is monitored by purity (dashed light blue lines) and average IPR in the sites basis (dashed-dotted red line). The histograms insets schematically represent the populations (not in scale) of the exciton on each site at a given time. (Right) The dependence of steady state delocalisation on the morphology is studied varying the standard deviation σ_θ of random torsional angles, and sampling 100 PPV polymers with 51 repeated units for each value of σ_θ .

$\langle eh | X_{\text{CoM}} | e'h' \rangle = \delta_{ee'} \delta_{hh'} (e + h)/2$, and $\langle eh | X_{\text{CS}} | e'h' \rangle = \delta_{ee'} \delta_{hh'} (e - h)$, as done in Ref. [31]. Alternatively, they can be expressed in terms of monomer coordinates $\vec{r}_k = (x_k, y_k, z_k)$, by replacing e (h) with a given Cartesian coordinate, such as x_e (x_h).

Localisation properties of Frenkel states are inferred from purity, $\mathcal{P}[\rho_t] = \text{Tr}[\rho_t^2]$, and average inverse participation ratio (IPR) [29, 34, 66, 94, 96]. Let $\rho = \sum_k p_k |r_k\rangle\langle r_k|$ be expressed in its eigenbasis $\{|r_k\rangle\}$, and let $\{|n\rangle\}$ be the sites basis then

$$\overline{\text{IPR}}(\rho) = \sum_k p_k \left(\sum_n |\langle n | r_k \rangle|^4 \right)^{-1}, \quad (16)$$

i.e., the weighted sum of the $\text{IPR} = 1/\sum_n |\langle n | \psi \rangle|^4$ for each pure state $|r_k\rangle$ making up the density operator ρ [34, 97]. From the IPR, delocalisation length can be estimated using $l = (\overline{\text{IPR}}(\rho))^{1/d}$ for a d -dimensional system [34]. Since the considered systems are either one-dimensional or ensembles of coupled one-dimensional systems we estimate the delocalisation length simply using $\overline{\text{IPR}}(\rho)$.

A. OPV hexamer

This system consists of six conjugated monomers and it is studied with a full Merrifield exciton approach, i.e., including all the possible CS states. For each morphology, we initialise the exciton in a Frenkel state localised on the *first* monomer. For comparison, a similar system was studied in Ref. [31] with a MCTDH method, requiring around 10^6 configurations for its numerical implementation, as opposed to the 36 required for the solution of Eq. (8) [98]

The crystalline morphology, shown in Fig. 2 (top), is obtained for a perfectly planar arrangement of the monomers

with constant bond-length alternation and no static disorder. It is characterised by trivial CS dynamics, which remains constant and equal to zero for all times. The exciton undergoes a initial ultrafast ballistic transport regime (1-10 fs), followed by a diffusive transport regime that lasts for the first 100 fs. During the evolution the partial states of electron and hole are perfectly symmetric, as shown in the histograms inset of Fig. 2 representing the population (not in scale) of the partial states of electron (black bars) and hole (light gray bars) on each site at a given time.

The semicrystalline morphology, an instance of which is shown in Fig. 2 (middle), is obtained for torsional angles normally distributed with standard deviation of 0.5 rad. The presence of disorder allows for a non trivial CS dynamics, thus reducing the energy barrier required for charge dissociation (CD) of the exciton. Despite the CoM dynamics has similar features to those of the crystalline morphology, asymmetry in the partial states of electron and hole is generally present both during the evolution and in the steady states.

The amorphous phase, an instance of which is shown in Fig. 2 (bottom), is obtained for torsional disorder with standard deviation of 1 rad. It is characterised by noticeable CS dynamics, with electron-hole separation over more than 2 monomers, lasting for hundreds of femtoseconds. Such CS dynamics can considerably reduce the CD energy for relatively long time spans of hundreds of femtoseconds. Remarkably, high-disorder allows for the formation of long-lived non-equilibrium states, before thermal equilibrium is reached around 100 ps. Exciton lifetimes may be shorter than the time required to reach thermal equilibrium in such systems. This implies that thermal equilibrium states of the excitons are generally not experimentally accessible.

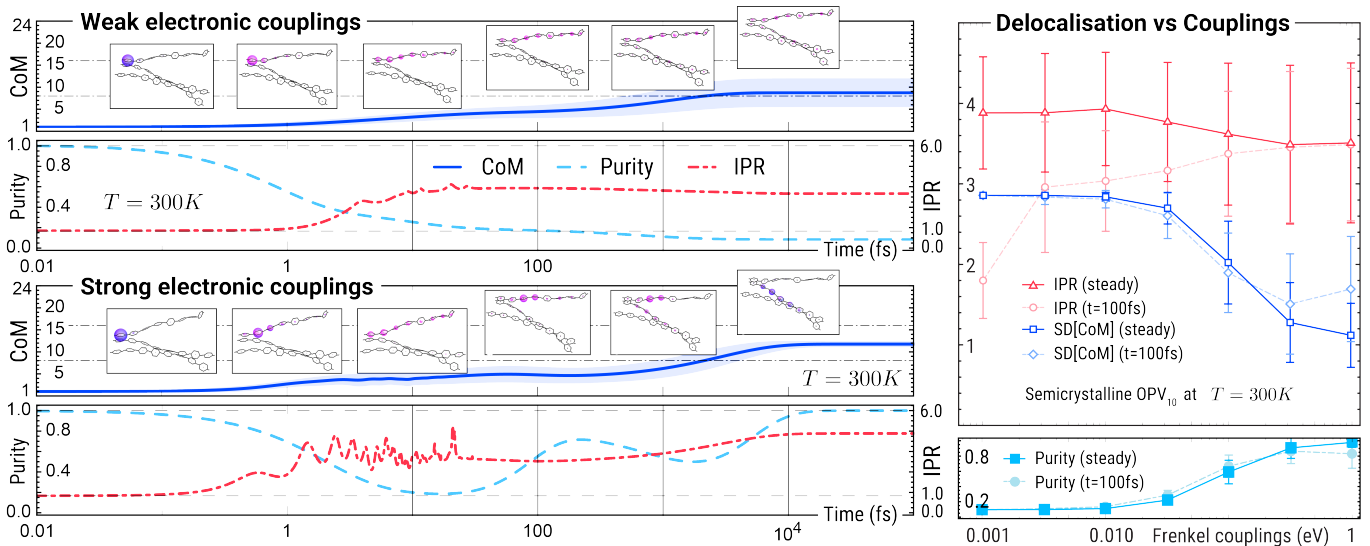


FIG. 4. (Left) Exciton transport for an arrangement of three semicrystalline OPV octamers with weak (10 – 100 meV) (top-left) and strong (0.1 – 1 eV) (bottom-left) electronic couplings at room temperature $T = 300K$. For each case the initial state ρ_0 is a Frenkel exciton localised on first monomer of the first octamer. Expectation value (solid lines) and standard deviation (shaded areas) of CoM (blue) are expressed in the sites basis. Delocalisation is monitored by purity (dashed light blue lines) and average IPR in the sites basis (dashed-dotted red line). The insets schematically represent the populations of the exciton on each site at a given time. (Right) The dependence of exciton delocalisation on the electronic couplings is studied varying the characteristic strength of Frenkel couplings from 10 meV to 1 eV. For each coupling regime we sampled 100 OPV oligomers with 10 repeated units and semicrystalline morphology ($\sigma_\theta = 0.5$ rad). Delocalisation is studied by evaluating IPR, purity and standard deviation of CoM for steady states and for states at 100 fs, with ρ_0 initialised in a Frenkel state localised on the first monomer.

B. PPV polymer

We now consider a PPV polymer with 51 repeated units. We restrict the dynamics to the Frenkel manifold to study the transport regimes of the CoM while limiting the computational cost. Excitons are here initialised in a Frenkel state localised on the *central monomer* ($k = 26$) of each considered polymer.

The crystalline morphology, shown in Fig. 3 (top-left), is characterised by a transition from ballistic to diffusive exciton transport during the first 100 fs, in analogy with the results of Ref. [19]. The remaining part of the dynamics consists in a relaxation process that guides the exciton towards thermal equilibrium. The absence of disorder in the sites energies and electronic couplings allows for the formation of highly delocalised steady states, with $\overline{\text{IPR}} > 30$.

However, in contrast with the results of Ref. [19], steady state populations are not evenly spread across the polymer, and thus only partially mixed. This is because the decoherence model used in Ref. [19] does not account for the spectral response between exciton coupling operators and the phonon bath. The results of Ref. [19] can be qualitatively reproduced using Eq. (8) by replacing the Lindblad operators $A_l(\omega)$ with the coupling operators A_l , and the associated relaxation rates $\gamma_l(\omega)$ with frequency independent rates γ_l . In such simplified limit, steady states become diagonal in the sites' basis. Here, instead, we use a Bloch-Redfield approach for rates and dissipators and obtain the correct thermal equilibrium states, which are diagonal in the exciton Hamiltonian basis.

As disorder is increased, localisation becomes more evident, undermining the ultrafast ballistic transport regime that would otherwise characterise a crystalline morphology. The amorphous morphology, an instance of which is shown in Fig. 3 (bottom-left), is characterised by sub-diffusive exciton transport within the first 100 fs, followed by thermal relaxation. States are remarkably less delocalised both during the dynamics and at equilibrium, with $\overline{\text{IPR}} \approx 6$ and CoM standard deviations much lower than for the crystalline morphology.

To further examine the relation between morphology and exciton delocalisation we study the IPR of steady states at room temperature for different morphological regimes. To do so we vary the standard deviation σ_θ for the random torsional angles between 0 (crystalline) and 1 rad (amorphous), sampling 100 different PPV polymers with 51 monomers for each morphology. The results, presented in Fig. 3 (right), show the high sensitivity of exciton delocalisation to conformational defects. Delocalisation rapidly drops from $\overline{\text{IPR}} \approx 35$ for crystalline polymers to $\overline{\text{IPR}} \approx 4$ for amorphous ones.

C. Dependence on electronic couplings

We now study the dynamics of Frenkel excitons for fixed morphology while varying the strength of the electronic couplings. This allows us to explore the different regimes of exciton transport and thermal equilibrium that are associated with weak (10 – 100 meV) or strong (0.1 – 1 eV) electronic

couplings. First, we illustrate such difference by looking at Frenkel exciton dynamics for a system given by three closely arranged OPV octamers that interact via through-space couplings, shown in Fig. 4 (*left*).

Systems characterised by weak electronic couplings rapidly lose their coherence, which vanishes within the first 10 – 20 fs. As shown in Fig. 4 (*top-left*), exciton transport is incoherent both during an initial intrachain transport over one oligomer and during the slower interchain transport across the different oligomers. The thermal energy is sufficient to populate several eigenstates of the exciton Hamiltonian. Thermal equilibrium is therefore characterised by low-purity and large CoM standard deviation.

Strong electronic couplings (≈ 1 eV) also display ultrafast intrachain dynamics, followed by a slower interchain transport. However, the thermal energy is not high enough to populate several states of the exciton Hamiltonian, therefore the steady states are rather pure and localised around the most energetically favourable clusters of conjugated monomers, as shown in Fig. 4 (*bottom-left*).

To systematically explore the dependence of exciton delocalisation on the strength of the electronic couplings (and thus on the thermal energy) we study IPR, purity and CoM standard deviation of transient (100 fs) and steady states of semicrystalline oligomers. The characteristic strength of Frenkel couplings is varied from 10 meV to 1 eV. For each coupling regime we sample 100 OPV oligomers with 10 repeated units and fixed semicrystalline morphology ($\sigma_\theta = 0.5$ rad). As shown in Fig. 4 (*right*), the average IPR decreases only slightly ($\approx 10\%$) over two orders of magnitude of electronic couplings strength. However, transport properties change dramatically, with CoM standard deviation and purity varying remarkably for both transient and steady states.

D. Final remarks

Using the model introduced in this article the dynamics of excitons in conjugated polymers is understood as a quantum thermalisation process, whose features strongly depend on the amount of disorder (i.e., morphology) and on the relative magnitude of thermal energy and electronic couplings (i.e., temperature). The non-equilibrium dynamics is characterised by an ultrafast and ballistic transport transient, followed by an intermediate diffusive or sub-diffusive process that occurs both through-bond and through-space. The dynamics culminates with thermal relaxation. Increasing disorder enables localisation, thus decreasing delocalisation lengths and IPR and hindering the efficacy of exciton transport. The amorphous phase is characterised by the presence of long-lived non-equilibrium states and prominent charge-separation dynamics, which however is limited to a few monomers, as previously reported in Ref. [24].

In polymers characterised by weak electronic couplings, of the order 10 – 100 meV, the environment *heats* the sys-

tem, driving the excitons low-purity thermal states, with non-negligible populations across the whole spectrum of energy eigenstates of the exciton Hamiltonian. Even though the intrinsic localisation lengths are low due to the presence of disorder, the thermal energy of the phonon bath (around 26 meV at room temperature) is sufficient to populate monomers that are far apart from the initial exciton location. In contrast, in materials characterised by strong Frenkel and charge-transfer couplings (≈ 1 eV), the phonon environment *cools* the system, leading the excitons to high-purity thermal state, with low-energy eigenstates of the exciton Hamiltonian being the only few populated ones. For this reason, despite the slower intrachain transport, systems with weak electronic couplings can display a more efficient transport mechanism over the picosecond time-scale at room temperature. This becomes particularly important for triplet excitons, which typically have lower mobility and longer lifetime than singlet excitons.

IV. CONCLUSIONS

In this article we have introduced a general master equation to study the dynamics of Merrifield excitons in conjugated polymers as a function of temperature and morphology of the medium. Using this method we have explored the general features of energy and charge transport in some representative systems based on PPV's electronic properties, confirming well known paradigms of quantum transport in disordered systems, and revealing non-equilibrium features such as long-lived states and charge-separation dynamics.

Beyond the qualitative understanding of exciton dynamics in amorphous polymers, we expect our method to be applicable for the quantitative study of energy and charge transport properties of specific materials. This can be done using a multi-scale approach based on molecular dynamics and first-principle calculations, as demonstrated in Refs. [19, 41, 42]. We also anticipate that this approach could be used to study disorder-dependent effects in OSCs, such as trapped-charge induced photoluminescence peak displacement [99, 100] and individual charge-carrier pathways in amorphous polymers [101].

ACKNOWLEDGMENTS

This research was supported by the Australian Research Council under grant number CE170100026. FC thanks Igor Lyskov and Ivan Kassal for insightful discussions. This research was undertaken with the assistance of resources from the National Computational Infrastructure (NCI), which is supported by the Australian Government. The authors acknowledge the people of the Woi wurrung and Boon wurrung language groups of the eastern Kulin Nations on whose unceded lands we work. We respectfully acknowledge the Traditional Custodians of the lands and waters across Australia and their Elders: past, present, and emerging.

- [1] H. Hoppe and N. S. Sariciftci, Polymer solar cells, *Advances in Polymer Science* **214**, 1–86 (2008).
- [2] S. Zhang, Y. Qin, J. Zhu, and J. Hou, Over 14% Efficiency in Polymer Solar Cells Enabled by a Chlorinated Polymer Donor, *Advanced Materials* **30** (2018).
- [3] G. Wang, F. S. Melkonyan, A. Facchetti, and T. J. Marks, All-Polymer Solar Cells: Recent Progress, Challenges, and Prospects, *Angewandte Chemie - International Edition* **58**, 4129–4142 (2019).
- [4] A. Zampetti, A. Minotto, and F. Cacialli, Near-Infrared (NIR) Organic Light-Emitting Diodes (OLEDs): Challenges and Opportunities, *Advanced Functional Materials* **29**, 1807623 (2019).
- [5] P. P. Manousiadis, K. Yoshida, G. A. Turnbull, and I. D. W. Samuel, Organic semiconductors for visible light communications, *Philosophical Transactions of the Royal Society A: Mathematical, Physical and Engineering Sciences* **378**, 20190186 (2020).
- [6] A. Salleo, M. L. Chabinyo, M. S. Yang, and R. A. Street, Polymer thin-film transistors with chemically modified dielectric interfaces, *Applied Physics Letters* **81**, 4383–4385 (2002).
- [7] J. H. Cho, J. Lee, Y. Xia, B. Kim, Y. He, M. J. Renn, T. P. Lodge, and C. Daniel Frisbie, Printable ion-gel gate dielectrics for low-voltage polymer thin-film transistors on plastic, *Nature Materials* **7**, 900–906 (2008).
- [8] H.-C. Wu, S. Rondeau-Gagné, Y.-C. Chiu, F. Lissel, J. W. F. To, Y. Tsao, J. Y. Oh, B. Tang, W.-C. Chen, J. B.-H. Tok, and Z. Bao, Enhanced Charge Transport and Stability Conferred by Iron(III)-Coordination in a Conjugated Polymer Thin-Film Transistors, *Advanced Electronic Materials* **4**, 1800239 (2018).
- [9] J. Zou, H. Wang, X. Zhang, X. Wang, Z. Shi, Y. Jiang, Z. Cui, and D. Yan, Polyimide-based gate dielectrics for high-performance organic thin film transistors, *Journal of Materials Chemistry C* **7**, 7454–7459 (2019).
- [10] V. Coropceanu, J. Cornil, D. A. da Silva Filho, Y. Olivier, R. Silbey, and J. L. Brédas, Charge transport in organic semiconductors, *Chemical Reviews* **107**, 926–952 (2007).
- [11] O. V. Mikhnenko, P. W. Blom, and T. Q. Nguyen, Exciton diffusion in organic semiconductors, *Energy and Environmental Science* **8**, 1867–1888 (2015).
- [12] H. Kang, S. Jung, S. Jeong, G. Kim, and K. Lee, Polymer-metal hybrid transparent electrodes for flexible electronics, *Nature Communications* **6**, 1–7 (2015).
- [13] H. Gao, J. Li, F. Zhang, Y. Liu, and J. Leng, The research status and challenges of shape memory polymer-based flexible electronics, *Materials Horizons* **6**, 931–944 (2019).
- [14] T. Brixner, R. Hildner, J. Köhler, C. Lambert, and F. Würthner, Exciton Transport in Molecular Aggregates - From Natural Antennas to Synthetic Chromophore Systems, *Advanced Energy Materials* **7**, 1700236 (2017).
- [15] S. J. Jang and B. Mennucci, Delocalized excitons in natural light-harvesting complexes, *Reviews of Modern Physics* **90**, 035003 (2018).
- [16] O. Ostroverkhova, Organic Optoelectronic Materials: Mechanisms and Applications, *Chemical Reviews* **116**, 13279–13412 (2016).
- [17] J. Aragón and A. Troisi, Dynamics of the excitonic coupling in organic crystals, *Physical Review Letters* **114**, 026402 (2015).
- [18] E. H. Horak, M. T. Rea, K. D. Heylman, D. Gelbwaser-Klimovsky, S. K. Saikin, B. J. Thompson, D. D. Kohler, K. A. Knapper, W. Wei, F. Pan, P. Gopalan, J. C. Wright, A. Aspuru-Guzik, and R. H. Goldsmith, Exploring Electronic Structure and Order in Polymers via Single-Particle Microresonator Spectroscopy, *Nano Letters* **18**, 1600–1607 (2018).
- [19] I. Lyskov, E. Trushin, B. Q. Baragiola, T. W. Schmidt, J. H. Cole, and S. P. Russo, First-Principles Calculation of Triplet Exciton Diffusion in Crystalline Poly(p-phenylene vinylene), *Journal of Physical Chemistry C* **123**, 26831–26841 (2019).
- [20] R. Binder and I. Burghardt, First-principles description of intra-chain exciton migration in an oligo(para-phenylene vinylene) chain. II. ML-MCTDH simulations of exciton dynamics at a torsional defect, *The Journal of chemical physics* **152**, 204120 (2020).
- [21] E. Collini and G. D. Scholes, Coherent intrachain energy migration in a conjugated polymer at room temperature, *Science* **323**, 369–373 (2009).
- [22] I. McCulloch, R. S. Ashraf, L. Biniek, H. Bronstein, C. Combe, J. E. Donaghey, D. I. James, C. B. Nielsen, B. C. Schroeder, and W. Zhang, Design of semiconducting indacenodithiophene polymers for high performance transistors and solar cells, *Accounts of Chemical Research* **45**, 714–722 (2012).
- [23] C. B. Nielsen, M. Turbiez, and I. McCulloch, Recent advances in the development of semiconducting DPP-containing polymers for transistor applications, *Advanced Materials* **25**, 1859–1880 (2013).
- [24] T. Qin and A. Troisi, Relation between structure and electronic properties of amorphous MEH-PPV polymers, *Journal of the American Chemical Society* **135**, 11247–11256 (2013).
- [25] L. C. Groff, X. Wang, and J. D. Mceill, Measurement of exciton transport in conjugated polymer nanoparticles, *Journal of Physical Chemistry C* **117**, 25748–25755 (2013).
- [26] H. Ma, T. Qin, and A. Troisi, Electronic excited states in amorphous MEH-PPV polymers from large-scale first principles calculations, *Journal of Chemical Theory and Computation* **10**, 1272–1282 (2014).
- [27] S. R. Yost, E. Hontz, S. Yeganeh, and T. Van Voorhis, Triplet vs singlet energy transfer in organic semiconductors: The tortoise and the hare, *Journal of Physical Chemistry C* **116**, 17369–17377 (2012).
- [28] V. Stehr, R. F. Fink, B. Engels, J. Pflaum, and C. Deibel, Singlet exciton diffusion in organic crystals based on marcus transfer rates, *Journal of Chemical Theory and Computation* **10**, 1242–1255 (2014).
- [29] J. J. Kranz and M. Elstner, Simulation of Singlet Exciton Diffusion in Bulk Organic Materials, *Journal of Chemical Theory and Computation* **12**, 4209–4221 (2016).
- [30] N. B. Taylor and I. Kassal, Generalised Marcus theory for multi-molecular delocalised charge transfer, *Chemical Science* **9**, 2942–2951 (2018).
- [31] R. Binder, J. Wahl, S. Römer, and I. Burghardt, Coherent exciton transport driven by torsional dynamics: A quantum dynamical study of phenylene-vinylene type conjugated systems, *Faraday Discussions* **163**, 205–222 (2013).
- [32] H. Oberhofer, K. Reuter, and J. Blumberger, Charge Transport in Molecular Materials: An Assessment of Computational Methods, *Chemical Reviews* **117**, 10319–10357 (2017).
- [33] R. Binder, D. Lauvergnat, and I. Burghardt, Conformational Dynamics Guides Coherent Exciton Migration in Conjugated Polymer Materials: First-Principles Quantum Dynamical Study, *Physical Review Letters* **120**, 227401 (2018).

- [34] D. Balzer, T. J. A. M. Smolders, D. Blyth, S. N. Hood, and I. Kassal, Delocalised kinetic Monte Carlo for simulating delocalisation-enhanced charge and exciton transport in disordered materials, *Chemical Science*, – (2021).
- [35] M. Mohseni, P. Rebentrost, S. Lloyd, and A. Aspuru-Guzik, Environment-assisted quantum walks in photosynthetic energy transfer, *Journal of Chemical Physics* **129**, 174106 (2008).
- [36] P. Rebentrost, M. Mohseni, I. Kassal, S. Lloyd, and A. Aspuru-Guzik, Environment-assisted quantum transport, *New Journal of Physics* **11**, 033003 (2009).
- [37] F. Caruso, A. W. Chin, A. Datta, S. F. Huelga, and M. B. Plenio, Highly efficient energy excitation transfer in light-harvesting complexes: The fundamental role of noise-assisted transport, *Journal of Chemical Physics* **131**, 105106 (2009).
- [38] F. Caruso, A. W. Chin, A. Datta, S. F. Huelga, and M. B. Plenio, Entanglement and entangling power of the dynamics in light-harvesting complexes, *Physical Review A - Atomic, Molecular, and Optical Physics* **81**, 062346 (2010).
- [39] S. Ohta, M. Nakano, R. Kishi, H. Takahashi, and S. Furukawa, Monte Carlo wavefunction approach to the exciton dynamics of molecular aggregates with exciton-phonon coupling, *Chemical Physics Letters* **419**, 70–74 (2006).
- [40] M. Nakano, S. Ito, T. Nagami, Y. Kitagawa, and T. Kubo, Quantum Master Equation Approach to Singlet Fission Dynamics of Realistic/Artificial Pentacene Dimer Models: Relative Relaxation Factor Analysis, *Journal of Physical Chemistry C* **120**, 22803–22815 (2016).
- [41] M. Nakano, Quantum master equation approach to singlet fission dynamics in pentacene ring-shaped aggregate models, *Journal of Chemical Physics* **150**, 234305 (2019).
- [42] X. Xie, A. Santana-Bonilla, W. Fang, C. Liu, A. Troisi, and H. Ma, Exciton-Phonon Interaction Model for Singlet Fission in Prototypical Molecular Crystals, *Journal of Chemical Theory and Computation* **15**, 3721–3729 (2019).
- [43] C. K. Lee, J. Moix, and J. Cao, Coherent quantum transport in disordered systems: A unified polaron treatment of hopping and band-like transport, *Journal of Chemical Physics* **142**, 164103 (2015).
- [44] M. B. Plenio and S. F. Huelga, Dephasing-assisted transport: Quantum networks and biomolecules, *New Journal of Physics* **10**, 113019 (2008).
- [45] I. Kassal, J. Yuen-Zhou, and S. Rahimi-Keshari, Does coherence enhance transport in photosynthesis?, *Journal of Physical Chemistry Letters* **4**, 362–367 (2013).
- [46] P. W. Anderson, Absence of diffusion in certain random lattices, *Physical Review* **109**, 1492–1505 (1958).
- [47] H. Wang, R. Marsh, J. P. Lewis, and R. A. Römer, Electronic transport and localization in short and long DNA, in *Modern Methods for Theoretical Physical Chemistry of Biopolymers* (Elsevier, 2006) pp. 407–427.
- [48] A. Lagendijk, B. Van Tiggelen, and D. S. Wiersma, Fifty years of Anderson localization, *Physics Today* **62**, 24–29 (2009).
- [49] M. Walschaers, J. F. D. C. Diaz, R. Mulet, and A. Buchleitner, Optimally designed quantum transport across disordered networks, *Physical Review Letters* **111**, 180601 (2013).
- [50] J. Jeske, N. Vogt, and J. H. Cole, Excitation and state transfer through spin chains in the presence of spatially correlated noise, *Physical Review A - Atomic, Molecular, and Optical Physics* **88**, 062333 (2013).
- [51] V. Gorini, A. Kossakowski, and E. C. Sudarshan, Completely positive dynamical semigroups of N-level systems, *Journal of Mathematical Physics* **17**, 821–825 (1975).
- [52] G. Lindblad, On the generators of quantum dynamical semigroups, *Communications in Mathematical Physics* **48**, 119–130 (1976).
- [53] D. A. Lidar, Z. Bihary, and K. B. Whaley, From completely positive maps to the quantum markovian semigroup master equation, *Chemical Physics* **268**, 35–53 (2001).
- [54] H.-P. Breuer and F. Petruccione, *The Theory of Open Quantum Systems* (Oxford University Press, 2002) p. 648.
- [55] S. Milz, F. A. Pollock, and K. Modi, An Introduction to Operational Quantum Dynamics, *Open Systems and Information Dynamics* **24** (2017).
- [56] V. Gowrishankar, S. R. Scully, M. D. McGehee, Q. Wang, and H. M. Branz, Exciton splitting and carrier transport across the amorphous-silicon/ polymer solar cell interface, *Applied Physics Letters* **89**, 252102 (2006).
- [57] V. Gowrishankar, S. R. Scully, A. T. Chan, M. D. McGehee, Q. Wang, and H. M. Branz, Exciton harvesting, charge transfer, and charge-carrier transport in amorphous-silicon nanopillar/polymer hybrid solar cells, *Journal of Applied Physics* **103**, 064511 (2008).
- [58] W. J. D. Beenken, Excitons in conjugated polymers: Do we need a paradigm change?, *Physica Status Solidi (A)* **206**, 2750–2756 (2009).
- [59] I. H. Nayyar, E. R. Batista, S. Tretiak, A. Saxena, D. L. Smith, and R. L. Martin, Localization of electronic excitations in conjugated polymers studied by DFT, *Journal of Physical Chemistry Letters* **2**, 566–571 (2011).
- [60] S. Kilina, N. Dandu, E. R. Batista, A. Saxena, R. L. Martin, D. L. Smith, and S. Tretiak, Effect of packing on formation of deep carrier traps in amorphous conjugated polymers, *Journal of Physical Chemistry Letters* **4**, 1453–1459 (2013).
- [61] R. S. Bhatta and M. Tsige, Chain length and torsional dependence of exciton binding energies in P3HT and PTB7 conjugated polymers: A first-principles study, *Polymer* **55**, 2667–2672 (2014).
- [62] M. T. Sajjad, A. J. Ward, C. Kästner, A. Ruseckas, H. Hoppe, and I. D. Samuel, Controlling Exciton Diffusion and Fullerene Distribution in Photovoltaic Blends by Side Chain Modification, *Journal of Physical Chemistry Letters* **6**, 3054–3060 (2015).
- [63] J. L. Brédas, E. H. Sargent, and G. D. Scholes, Photovoltaic concepts inspired by coherence effects in photosynthetic systems, *Nature Materials* **16**, 35–44 (2016).
- [64] L. Simine and P. J. Rossky, Relating Chromophoric and Structural Disorder in Conjugated Polymers, *Journal of Physical Chemistry Letters* **8**, 1752–1756 (2017).
- [65] R. Noriega, Efficient Charge Transport in Disordered Conjugated Polymer Microstructures, *Macromolecular Rapid Communications* **39**, 1800096 (2018).
- [66] G. D. Scholes, Limits of exciton delocalization in molecular aggregates, *Faraday Discussions* **221**, 265–280 (2019).
- [67] R. Pandya, A. M. Alvertis, Q. Gu, J. Sung, L. Legrand, D. Kréher, T. Barisien, A. W. Chin, C. Schnedermann, and A. Rao, How Does the Symmetry of S1 Influence Exciton Transport in Conjugated Polymers?, [arXiv:2010.03888](https://arxiv.org/abs/2010.03888) (2020).
- [68] R. E. Merrifield, Ionized states in a one-dimensional molecular crystal, *The Journal of Chemical Physics* **34**, 1835–1839 (1961).
- [69] J. Frenkel, On the transformation of light into heat in solids. II, *Physical Review* **37**, 1276–1294 (1931).
- [70] J. Jeske, D. J. Ing, M. B. Plenio, S. F. Huelga, and J. H. Cole, Bloch-Redfield equations for modeling light-harvesting complexes, *Journal of Chemical Physics* **142**, 064104 (2015).
- [71] F. E. Figueirido and R. M. Levy, Vibrational relaxation and

- Bloch-Redfield theory, *The Journal of Chemical Physics* **97**, 703–706 (1992).
- [72] D. A. Lidar and K. Birgitta Whaley, *Decoherence-Free Subspaces and Subsystems* (Springer Berlin Heidelberg, Berlin, Heidelberg, 2003) pp. 83–120.
- [73] F. Binder, S. Vinjanampathy, K. Modi, and J. Gool, Quantum thermodynamics of general quantum processes, *Physical Review E - Statistical, Nonlinear, and Soft Matter Physics* **91**, 032119 (2015).
- [74] J. D. Whitfield, C. A. Rodríguez-Rosario, and A. Aspuru-Guzik, Quantum stochastic walks: A generalization of classical random walks and quantum walks, *Physical Review A - Atomic, Molecular, and Optical Physics* **81**, 022323 (2010).
- [75] I. Sinayskiy and F. Petruccione, Open quantum walks: A mini review of the field and recent developments, *European Physical Journal: Special Topics* **227**, 1869–1883 (2019).
- [76] Also known as Gorini–Kossakowski–Sudarshan–Lindblad (GKSL) master equation [55].
- [77] R. S. Sánchez-Carrera, P. Paramonov, G. M. Day, V. Coropceanu, and J. L. Brédas, Interaction of charge carriers with lattice vibrations in oligoacene crystals from naphthalene to pentacene, *Journal of the American Chemical Society* **132**, 14437–14446 (2010).
- [78] M. Walschaers, F. Schlawin, T. Wellens, and A. Buchleitner, Quantum Transport on Disordered and Noisy Networks: An Interplay of Structural Complexity and Uncertainty, *Annual Review of Condensed Matter Physics* **7**, 223–248 (2016).
- [79] C. Dittel, G. Dufour, M. Walschaers, G. Weihs, A. Buchleitner, and R. Keil, Totally Destructive Many-Particle Interference, *Physical Review Letters* **120**, 240404 (2018).
- [80] J. Jeske and J. H. Cole, Derivation of Markovian master equations for spatially correlated decoherence, *Physical Review A - Atomic, Molecular, and Optical Physics* **87**, 052138 (2013).
- [81] C. Batey, J. Jeske, and A. D. Greentree, Dark State Adiabatic Passage with Branched Networks and High-Spin Systems: Spin Separation and Entanglement, *Frontiers in ICT* **2**, 19 (2015).
- [82] M. Grover and R. Silbey, Exciton migration in molecular crystals, *The Journal of Chemical Physics* **54**, 4841–4843 (1971).
- [83] V. Pouthier, Multi-quanta energy relaxation in a nonlinear quantum dimer coupled to a phonon bath, *Physica D: Nonlinear Phenomena* **221**, 13–30 (2006).
- [84] S. Jang, Y. C. Cheng, D. R. Reichman, and J. D. Eaves, Theory of coherent resonance energy transfer, *Journal of Chemical Physics* **129**, 101104 (2008).
- [85] D. P. McCutcheon and A. Nazir, Coherent and incoherent dynamics in excitonic energy transfer: Correlated fluctuations and off-resonance effects, *Physical Review B - Condensed Matter and Materials Physics* **83**, 165101 (2011).
- [86] S. Athanasopoulos, J. Kirkpatrick, D. Martínez, J. M. Frost, C. M. Foden, A. B. Walker, and J. Nelson, Predictive study of charge transport in disordered semiconducting polymers, *Nano Letters* **7**, 1785–1788 (2007).
- [87] V. Janković and N. Vukmirović, Energy-Temporal Pathways of Free-Charge Formation at Organic Bilayers: Competition of Delocalization, Disorder, and Polaronic Effects, *Journal of Physical Chemistry C* **124**, 4378–4392 (2020).
- [88] F. Ortmann, F. Bechstedt, and K. Hannewald, Theory of charge transport in organic crystals: Beyond Holstein’s small-polaron model, *Physical Review B - Condensed Matter and Materials Physics* **79**, 235206 (2009).
- [89] I. I. Fishchuk, A. Kadashchuk, S. T. Hoffmann, S. Athanasopoulos, J. Genoe, H. Bäessler, and A. Köhler, Unified description for hopping transport in organic semiconductors including both energetic disorder and polaronic contributions, *Physical Review B - Condensed Matter and Materials Physics* **88**, 125202 (2013).
- [90] E. Y. Wilner, H. Wang, M. Thoss, and E. Rabani, Sub-Ohmic to super-Ohmic crossover behavior in nonequilibrium quantum systems with electron-phonon interactions, *Physical Review B - Condensed Matter and Materials Physics* **92**, 195143 (2015).
- [91] S. Takahashi, K. Watanabe, and Y. Matsumoto, Singlet fission of amorphous rubrene modulated by polaron formation, *Journal of Chemical Physics* **151** (2019).
- [92] T. Nelson, S. Fernandez-Alberti, A. E. Roitberg, and S. Tretiak, Electronic Delocalization, Vibrational Dynamics, and Energy Transfer in Organic Chromophores, *Journal of Physical Chemistry Letters* **8**, 3020–3031 (2017).
- [93] S. Lefrant, E. Perrin, J. P. Buisson, H. Eckhardt, and C. C. Han, Vibrational studies of polyparaphenylene-vinylene (PPV), *Synthetic Metals* **29**, 91–96 (1989).
- [94] T. E. Dykstra, E. Hennebicq, D. Beljonne, J. Gierschner, G. Claudio, E. R. Bittner, J. Knoester, and G. D. Scholes, Conformational disorder and ultrafast exciton relaxation in PPV-family conjugated polymers, *Journal of Physical Chemistry B* **113**, 656–667 (2009).
- [95] T. F. Havel, Robust procedures for converting among Lindblad, Kraus and matrix representations of quantum dynamical semigroups, *Journal of Mathematical Physics* **44**, 534–557 (2003).
- [96] M. Cho, H. M. Vaswani, T. Brixner, J. Stenger, and G. R. Fleming, Exciton analysis in 2D electronic spectroscopy, *Journal of Physical Chemistry B* **109**, 10542–10556 (2005).
- [97] J. M. Moix, M. Khasin, and J. Cao, Coherent quantum transport in disordered systems: I. the influence of dephasing on the transport properties and absorption spectra on one-dimensional systems, *New Journal of Physics* **15**, 085010 (2013).
- [98] As discussed in Sec. II this advantage in terms of computational cost comes at the expense of several approximations that reduce the accuracy of the master equation.
- [99] C. Bardeen, Exciton quenching and migration in single conjugated polymers, *Science* **331**, 544–545 (2011).
- [100] J. C. Bolinger, M. C. Traub, T. Adachi, and P. F. Barbara, Ultralong-range polaron-induced quenching of excitons in isolated conjugated polymers, *Science* **331**, 565–567 (2011).
- [101] K. Wilma, A. Issac, Z. Chen, F. Würthner, R. Hildner, and J. Köhler, Tracing Single Electrons in a Disordered Polymer Film at Room Temperature, *Journal of Physical Chemistry Letters* **7**, 1478–1483 (2016).